Clim Dyn (2017) 49:1665–1679
DOI 10.1007/s00382-016-3411-1

WES feedback and the Atlantic Meridional Mode: observations and CMIP5 comparisons

Dillon J. Amaya[1] · Michael J. DeFlorio[2] · Arthur J. Miller[1] · Shang-Ping Xie[1]

Received: 21 April 2016 / Accepted: 15 October 2016 / Published online: 25 October 2016

Abstract The Atlantic Meridional Mode (AMM) is the dominant mode of tropical SST/wind coupled variability. Modeling studies have implicated wind-evaporation-SST (WES) feedback as the primary driver of the AMM's evolution across the Atlantic basin; however, a robust coupling of the SST and winds has not been shown in observations. This study examines observed AMM growth, propagation, and decay as a result of WES interactions. Investigation of an extended maximum covariance analysis shows that boreal wintertime atmospheric forcing generates positive SST anomalies (SSTA) through a reduction of surface evaporative cooling. When the AMM peaks in magnitude during spring and summer, upward latent heat flux anomalies occur over the warmest SSTs and act to dampen the initial forcing. In contrast, on the southwestern edge of the SSTA, SST-forced cross-equatorial flow reduces the strength of the climatological trade winds and provides an anomalous latent heat flux into the ocean, which causes southwestward propagation of the initial atmosphere-forced SSTA through WES dynamics. Additionally, the lead-lag relationship of the ocean and atmosphere indicates a transition from an atmosphere-forcing-ocean regime in the northern subtropics to a highly coupled regime in the northern tropics that is not observed in the southern hemisphere. CMIP5 models poorly simulate the latitudinal transition from a one-way interaction to a two-way feedback, which may explain why they also struggle to reproduce spatially coherent interactions between tropical Atlantic SST and winds. This analysis provides valuable insight on how meridional modes act as links between extratropical and tropical variability and focuses future research aimed at improving climate model simulations.

Keywords Atlantic Meridional Mode · WES feedback · CMIP5 · Air-sea interactions · Maximum covariance analysis

1 Introduction

Interannual variability of the tropical Atlantic coupled ocean–atmosphere system is most significantly influenced by two modes of climate: the Atlantic Niño (Zebiak 1993) and the Atlantic Meridional Mode (AMM; Chiang and Vimont 2004). The Atlantic Niño is an El Niño-Southern Oscillation (ENSO)-like response to zonal movement of the equatorial thermocline, which produces anomalous sea surface temperatures (SST) and significant shifts in the Atlantic Walker and Hadley Circulations. This response is phase-locked to boreal summer and is driven by Bjerknes dynamics that are also associated with the Pacific ENSO (e.g., Zebiak 1993; Carton and Huang 1994). The Atlantic Meridional Mode involves interannual and decadal fluctuations of the interhemispheric SST gradient in the tropical Atlantic, which drives cross-equatorial boundary layer flow toward the anomalously warm hemisphere (Nobre and Shukla 1996; Chang et al. 1997). This fluctuation of the meridional SST gradient significantly modulates the seasonal march of the Intertropical Convergence Zone (ITCZ), which impacts regional rainfall over Northeast Brazil and the Sahel of Africa (Foltz et al. 2012; Xie and Carton 2004;

✉ Dillon J. Amaya
djamaya@ucsd.edu

[1] Scripps Institution of Oceanography, University of California-San Diego, 9500 Gilman Drive #0206, La Jolla, CA 92093-0206, USA

[2] Jet Propulsion Laboratory, California Institute of Technology, M/S 300-323, 4800 Oak Grove Drive, Pasadena, CA 91109, USA

Hastenrath and Heller 1977; Folland et al. 1986). In addition, the AMM has been shown to affect Atlantic hurricane activity (e.g., Vimont and Kossin 2007).

Several hypotheses have been proposed to explain the dynamical genesis of the AMM. Nobre and Shukla (1996) first suggested an external mechanism in which trade wind variations in the tropical north Atlantic force SST anomalies (SSTA) through surface latent heat flux anomalies. In subsequent studies, ENSO and the North Atlantic Oscillation (NAO) were identified as examples of large-scale climate modes which can cause remotely forced and stochastically generated trade wind variations that give rise to a meridional SST asymmetry about the equator (e.g., Chiang et al. 2002; Amaya and Foltz 2014).

A second mechanism outlined by Chang et al. (1997) implicates wind-evaporation-SST (WES) feedback (Xie and Philander 1994) as the major mechanism for the AMM. In this theory, cross-equatorial atmospheric flow reduces the strength of the trade winds in the warmer hemisphere and increases the strength of the trades in the cooler hemisphere due to turning by the Corolis force. This change in the magnitude of the trade winds acts to reinforce the meridional SST gradient through anomalous, opposite signed surface evaporation between hemispheres. Several studies have also indicated that tropical and subtropical low-level cloud cover anomalies can force changes in SST anomalies, and consequently affect the meridional SST gradient, due to enhanced shortwave reflection (e.g., Evan et al. 2013; Tanimoto and Xie 2002). The ITCZ, which is sensitive to variations in this meridional gradient, then follows the SST patterns and trade wind convergences into the warmer hemisphere (Chiang et al. 2002).

However, subsequent studies have shown that WES feedback is largely confined to the deep tropics and is relatively weak, requiring at least some external forcing to sustain the coupled variability and reproduce the observed AMM behavior (Chang et al. 2001; Chiang et al. 2002; Czaja et al. 2002). In particular, Chang et al. (2001) used a 145-year simulation of an atmospheric general circulation model (AGCM) to show that stochastic forcing alone can generate significant SSTA in the tropical Atlantic north of about 15°N, but a weak-to-moderate local air-sea coupling is needed to reproduce observed tropical Atlantic variability south of this latitude.

In spite of the many advances made by these studies, there is still widespread uncertainty regarding the role of WES feedback in exciting and sustaining the AMM. Chang et al. (2001) presented observational evidence in support of the WES feedback theory based on a lagged correlation analysis between different time series in a maximum covariance analysis (MCA). Similarly, Sutton et al. (2000) and Okumura et al. (2001) examined the AMM in a modeling framework and found a negative and slightly positive WES feedback, respectively, through model analysis, while Ruiz-Barradas et al. (2003) showed a positive feedback throughout the north tropical Atlantic, except off the coast of Africa. These studies were primarily based on the outputs of AGCMs, which can produce different feedback strengths among models (Frankignoul et al. 2004). Wary of model uncertainty, Frankignoul and Kestenare (2005) conducted a study based on observational reanalysis data aimed at revisiting air-sea coupled interactions in the tropical Atlantic. They showed that boreal winter trade wind anomalies north of approximately 10°N off the coast of Africa can generate initial SSTAs through anomalous latent heat fluxes, which are then sustained in the deep tropics by positive WES feedback.

Very few studies have investigated how initial stochastically forced SST anomalies in the subtropics evolve into a fully coupled ocean–atmosphere thermodynamic mode in the deeper tropics. Such an analysis would complement many of the previous investigations mentioned here, which focused on the AMM/WES feedback relationship in the context of mechanistic generation and sustention. WES feedback theory suggests that a positive SST anomaly will propagate southwestward due to the tendency of SST-forced surface wind anomalies to weaken (strengthen) the climatological trade winds on the southwestern (northeastern) edge of the SST anomaly, potentially providing the link from subtropical origins to deep tropical growth and decay (e.g., Xie 1999).

In the Pacific, Vimont et al. (2001, 2003) expanded upon this idea and proposed a seasonal footprinting mechanism by which mid-latitude atmospheric variability during boreal winter could potentially force a subtropical SST anomaly that would then propagate through WES feedback to the equatorial Pacific in the summer and influence zonal surface wind and SST variability. Subsequent modeling efforts by Vimont (2010), Vimont et al. (2009), and Wu et al. (2010) confirmed that WES feedback could indeed propagate subtropical Pacific SSTA southwestward toward the central Pacific, though in some cases over much faster timescales than originally proposed. These results have informed recent studies which indicate that the AMM and its Pacific counterpart (the Pacific Meridional Mode, PMM) may act as conduits by which extratropical atmospheric variability can significantly influence equatorial SST variability, thereby exciting Atlantic Niño and Pacific ENSO events through this WES-driven propagation (Vimont et al. 2003; Foltz and McPhaden 2010; Alexander et al. 2010; Larson and Kirtman 2014; Di Lorenzo and Mantua 2016).

While the WES driven propagation of anomalies associated with the PMM has been well studied over recent years, there remains little observational evidence of a similar mechanistic evolution of the AMM. In this study, we use observations to synthesize the results outlined by the

previous literature and paint a consistent and cohesive picture of WES dynamics in the tropical Atlantic as it pertains to AMM generation, propagation, and decay. We then use this new observational insight to test the performance of models included in phase 5 of the Coupled Model Intercomparison Project (CMIP5) in simulating AMM structure and the physical mechanisms associated with its propagation. While individual CMIP5 models have been used to evaluate the physical mechanisms governing AMM variability, a full comparison of a suite of CMIP5 models has not been investigated. Our observational and model results bring together nearly two decades of research in tropical Atlantic coupled variability and could potentially increase predictability and prediction skill of the AMM in future modeling efforts, benefiting socioeconomic endeavors in coastal Atlantic countries that are affected by interannual climate variability.

In the following section, we outline the observational data sets employed in our study, as well as the specifications for the CMIP5 models being evaluated. Sections 3 and 4 consist of our observational analysis of the AMM's spatiotemporal evolution. In Sect. 5, we repeat the analysis performed in Sects. 3 and 4, but for a suite of CMIP5 models. Section 6 contains a summary and accompanying discussion of our results.

2 Data and methods

We characterize tropical Atlantic SST variability using monthly mean data from the National Oceanic and Atmospheric Administration's Extended Reconstructed Sea Surface Temperature Version 3b (NOAA ERRST.v3b), which is available from 1854-present (Smith et al. 2008). We limit our analysis to 1950-2015, since the spatial density of SST data increased significantly during this period. Monthly mean 10-m wind and net surface latent heat flux data are obtained from the National Centers for Environmental Prediction-National Center for Atmospheric Research (NCEP-NCAR) Reanalysis (Kalnay et al. 1996), also from January 1950 to December 2015. We find that our results are largely insensitive to the choice of a particular reanalysis product.

We investigate tropical Atlantic coupled variability by applying a maximum covariance analysis (MCA; Bretherton et al. 1992) between SST and both components of the 10-m horizontal wind. MCA is analogous to empirical orthogonal function (EOF) analysis, but performs the singular value decomposition on the cross-covariance matrix between the variables. The resulting expansion coefficients (ECs) associated with the left and right singular vectors can then be projected onto the original data to obtain homogeneous and heterogeneous regression maps. The MCA results in this study show the homogeneous SST structure and the heterogeneous surface horizontal wind structure, so that both regressions are the result of the same time variability.

The AMM spatiotemporal evolution is examined using an extended MCA (EMCA) technique, which incorporates time-lagged information, similar to the technique used by Frankignoul and Kestenare (2005) and Polo et al. (2008). The EMCA methodology is largely similar to MCA, but differs in that seasonally averaged time series of SST and 10-m wind anomalies are stacked before computing the cross-covariance matrix, such that December–February (DJF) averaged maps are on top of March–May (MAM), June–August (JJA), and September–November (SON) averaged maps. Thus, if the data initially had dimensions of $N \times M$, where N is the time dimension and M is space, it has dimensions $N \times 4{*}M$ after stacking the matrices. The cross-covariance matrix is then calculated and the singular value decomposition is performed on this new matrix. EMCA yields four spatial structures per variable which are lagged in time, but are all described by a single EC.

Model evaluation is based on historical simulations of 17 CMIP5 models. The modeling centers and countries, CMIP5 model abbreviations, and the number of runs for each model used in this study are shown in Table 1. Monthly mean SST, 10-m winds, and net surface latent heat flux were used from 1950 to 2005 for each model. For brevity we show only the multi-model mean results. The MCA and various regressions were performed for each model separately and the average spatial pattern for the respective variables was taken to be the multi-model mean. For models with multiple ensemble members, each member was stacked in time such that the stacked array would have dimensions of $N{*}(\textit{number of ensembles}) \times M$. The MCA and other analyses were then calculated based on this stacked matrix.

Prior to MCA analyses, all fields are linearly detrended. Data used to calculate Fig. 1 are smoothed with a 3-month running mean at each grid point. Additionally, we remove the linear influence of ENSO on tropical Atlantic coupled variability by regressing out the cold tongue index (CTI; 6°N–6°S, 180°W–90°W) from each field at each grid point for data used in Figs. 1, 2, 3, 5, 6 and 7. Monthly anomalies in the observational analysis are relative to the climatology 1986–2015, while CMIP5 evaluations are relative to 1976–2005.

3 AMM propagation in observations

Following Chiang and Vimont (2004), we first apply MCA analysis to observed SST and 10-m winds in the domain 32°N–22°S and 74°W to the African coastline. The leading mode of tropical Atlantic coupled SST/wind variability

Table 1 The modeling center, country, model abbreviation, and number of ensemble members for each CMIP5 model used in this analysis

Modeling center	CMIP5 model abbreviations	Number of runs
Centre for Australian Weather and Climate Research, Australia	ACCESS1-0	1
	ACCESS1-3	2
College of Global Change and Earth System Science, China	BNU-ESM	1
Centre for Meteorological Research, France	CNRM-CM5	10
Geophysical Fluid Dynamics Laboratory, USA	GFDL-ESM2G	1
	GFDL-ESM2 M	1
Institute for Numerical Mathematics, Russia	INM-CM4	1
Institute Pierre Simon Laplace, France	IPSL-CM5A-LR	6
	IPSL-CM5A-MR	3
	IPSL-CM5B-LR	1
University of Tokyo/NIES/JAMSTEC, Japan	MIROC5	5
Max Planck Institute for Meteorology, Germany	MPI-ESM-LR	3
	MPI-ESM-P	2
Meteorological Research Institute, Japan	MRI-CGCM3	5
	MRI-ESM1	1
Norwegian Climate Centre, Norway	NorESM1-M	3
	NorESM1-ME	1

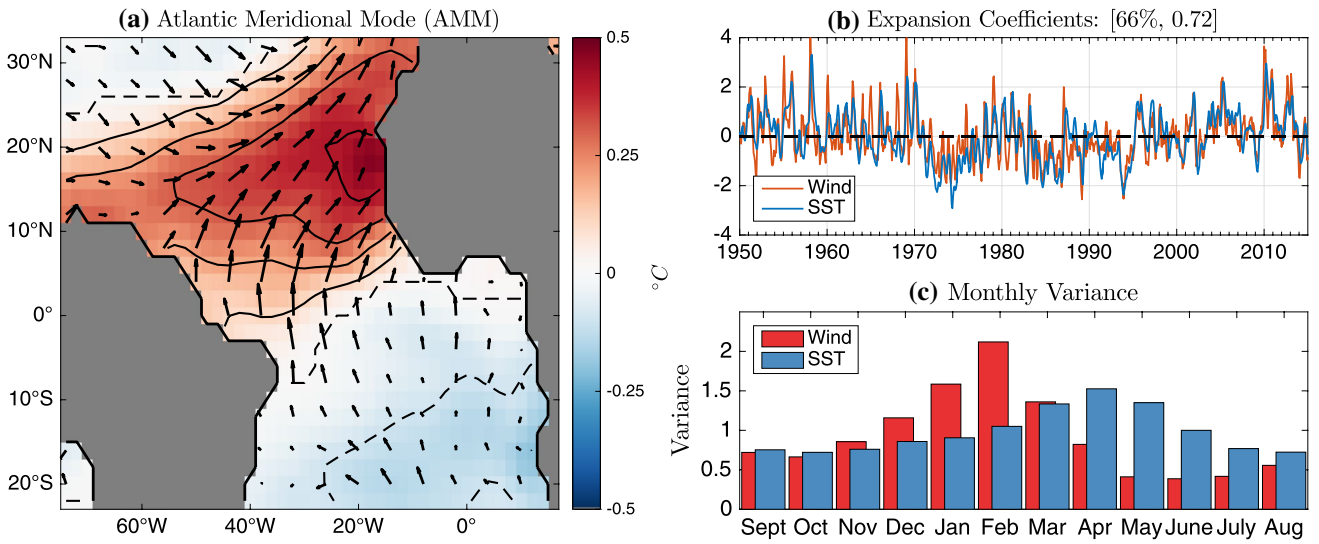

Fig. 1 **a** The observed leading maximum covariance analysis (MCA) mode of SSTA (*shading*, °C) and 10-m wind anomalies (*arrows*, m/s). **b** The corresponding left and right normalized expansion coefficients (EC). The *first number* in the *brackets* is the squared covariance fraction for the leading MCA mode; the *second number* is the correlation between the two ECs. **c** Month-to-month variance of the wind EC (*red*) and SST EC (*blue*)

is shown in Fig. 1a, while the normalized ECs, which describe the time variability of the leading spatial modes, are shown in Fig. 1b. The squared covariance fraction for the leading mode is 66% and the correlation coefficient of the two ECs is 0.72, indicating strong coupling of SST and winds in this region.

The leading mode of covariability in the tropical Atlantic is the AMM (Fig. 1a). There is a strong interhemispheric asymmetry in SSTA spatial loading, with positive values in the northern hemisphere (NH) and lower magnitude negative values in the southern hemisphere (SH), which is consistent with previous results (e.g., Chiang and Vimont 2004). From approximately 25°N to 5°N, strong southwesterly wind anomalies are co-located with the strongest SSTAs, centered at about 20°W. There are also cross-equatorial winds that begin as southeasterly flow just south of

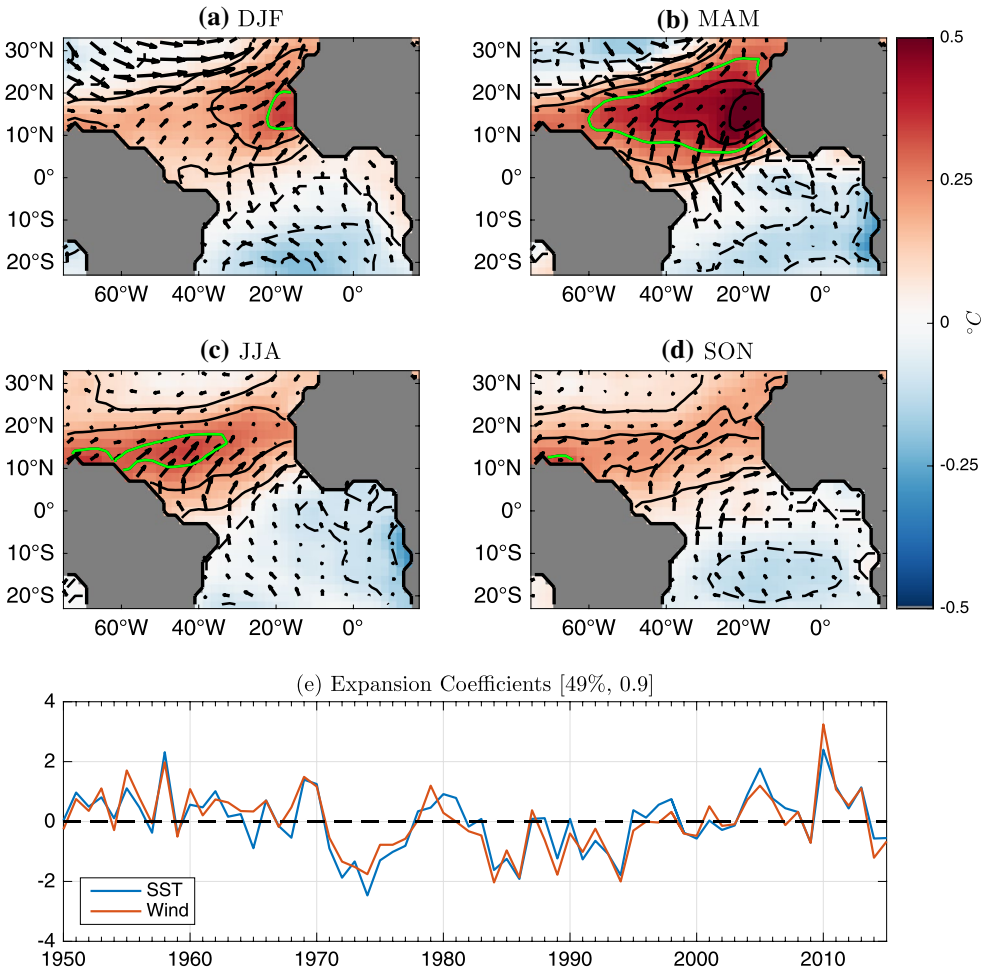

Fig. 2 **a–d** The observed leading extended maximum covariance analysis (EMCA) mode of SSTA (*shading*/*contours*, °C) and 10-m wind anomalies (*arrows*, m/s). The contour interval is 0.1 °C and the *green line* represents the 0.3 °C contour. **e** The corresponding left and right normalized expansion coefficients (EC). The *first number* in the *brackets* is the squared covariance fraction for the leading EMCA mode. The *second number* is the correlation between the two ECs, which indicates the strength of coupling between SST and winds in this region

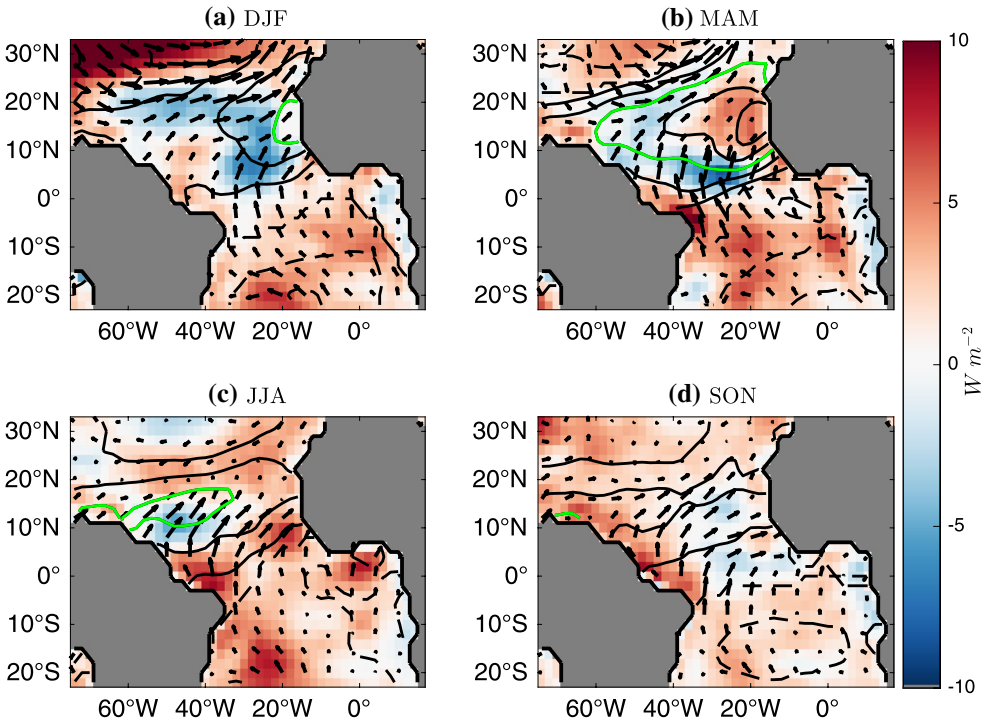

Fig. 3 Regression of observed net surface latent heat flux (positive upward, *shading*, Wm^{-2}) and 10-m winds (*arrows*, m/s) onto the SST expansion coefficient in Fig. 2e. Contours are the EMCA SSTA values shown in Fig. 2. The contour interval is 0.1 °C and the *green line* represents the 0.3 °C contour

the equator, turning to southwesterly flow just north of the equator. This C-shape bend in the winds about the equator is a distinct signature of WES feedback and will be analyzed in more detail in Sect. 4.

The ECs depicted in Fig. 1b vary on interannual to multidecadal timescales. In particular, the low-frequency component of the AMM ECs is reminiscent of the Atlantic Multidecadal Oscillation (AMO) index, which is well-correlated with both the SST and wind ECs (0.72 and 0.46 correlation coefficients, respectively). The surface wind variability associated with the AMM peaks in late boreal winter, while the SSTA structure peaks in the spring (Fig. 1c). Atmospheric variability leading SSTA variability by about a season is generally consistent with stochastic atmospheric forcing of a subsequently sustained SST anomaly (e.g., Chang et al. 2001).

MCA extracts the leading mode of coupled variability between the input variables, independent of the temporal evolution of the mode itself. Consequently, the mode depicted in Fig. 1a spans the entire AMM life cycle and consolidates its genesis, growth, and decay into one single mode (Chiang and Vimont 2004). To isolate these individual stages of the AMM, we compute the leading EMCA (see Sect. 2) mode of the SSTA and 10-m surface winds (Fig. 2). The squared covariance fraction for this mode is 49% and the correlation of the left and right ECs is 0.9. The observed surface latent heat flux was then regressed onto the resulting SST EC depicted in Fig. 2e, and the results are shown in Fig. 3. In Figs. 2 and 3, the SSTA are contoured in black and the 0.3 °C contour is outlined in green. The convention for latent heat flux anomalies in Fig. 3 is such that a positive (negative) anomaly corresponds to an upward (downward) energy flux and a cooling (warming) of the ocean.

In DJF, there are strong westerly surface wind anomalies in the NH subtropics from 32°N to 20°N (Fig. 2a). These surface wind anomalies lie on the northern edge of a band of positive SSTA that runs from the west coast of Africa to the north/northeast coast of South America. A localized maximum in SSTA can be seen centered on 15°N, 18°W (green contour). In Fig. 3a, we observe three distinct forcing regimes that give rise to the SSTAs described in Fig. 2a. The first regime is characterized by a tongue of negative latent flux anomalies extending from 20°N to 10°N and 60°W to 20°W. These anomalies increase in magnitude going from west-to-east toward more positive SSTA (black contours) and are generally co-located with strong westerly surface wind anomalies at 20°N. This co-location is consistent with boreal wintertime atmospheric forcing associated with NAO variability which reduces the strength of the background trade winds in the NH, thereby reducing evaporative cooling at the surface and driving an anomalous flux of latent energy into the ocean.

The second forcing regime is associated with cross-equatorial flow that turns southwesterly in the NH, driving negative latent heat flux anomalies that extend from 20°N to the equator at around 30°W (Figs. 2a, 3a). These anomalies are found on the southwest edge of the SSTA warm pool and are an early indication of air-sea interactions associated with WES feedback. The final regime is centered on the SSTA maximum outlined by the green contour. Here, southwesterly anomalies oppose the climatological upwelling favorable winds along the African coastline, which may weaken coastal upwelling and provide a latent heat flux which dampens co-located SSTAs. A flux of energy into the ocean on the west/southwest edge of the SSTA warm pool coupled with a near zero latent heat flux in the center of the SSTA maximum would lead to a propagation of the SSTA west/southwestward in the following season, representing AMM genesis.

The leading mode of SST and wind covariability during MAM (Fig. 2b) is much more pronounced in magnitude and spatial extent. Consequently, the MAM spatial structure most closely resembles the spatial structure of the "all-months" AMM shown in Fig. 1a. The NAO-like forcing regime seen in DJF appears to have weakened significantly in the NH subtropics with near zero flow over the warmest SSTAs. The SSTA maximum has extended southwest as far as 60°W, which is consistent with the energy fluxes observed in DJF (Fig. 2b, green contour). Despite this propagation, the local SSTA maximum in MAM is still located just off the coast of Africa and is likely due to the persistence of stochastic atmospheric forcing throughout boreal winter into early spring. In addition, the WES feedback regime has enhanced significantly as the weak cross-equatorial flow seen in DJF has increased in magnitude and extended across the basin west of 15°W in MAM. This anomalous boundary layer flow is southeasterly from 0° to 10°S and southwesterly from 0° to 10°N and is representative of a locally driven ocean-forced response in the surface winds (Fig. 4). The exact nature of the transition to an ocean-forced wind change as a function of latitude will be described in Sect. 4.

The regression of latent heat flux anomalies onto the SST EC shows negative values (ocean warming) that are closely co-located with the 0.3 °C green contour and the most significant southwesterly wind anomalies (Fig. 3b). In contrast, there are very weak surface wind anomalies and positive latent heat flux anomalies over the warmest SSTA anomalies (marked by the 0.4 and 0.5 °C contours; Figs. 2b and 3b). These localized positive latent heat flux anomalies are likely due to warm SST generating small-scale convection, which would lift warm air from the boundary layer and act as a damping on the SSTA in the region. This zonal dipole of latent heat flux anomalies is consistent with WES feedback theory and illustrates the competition between

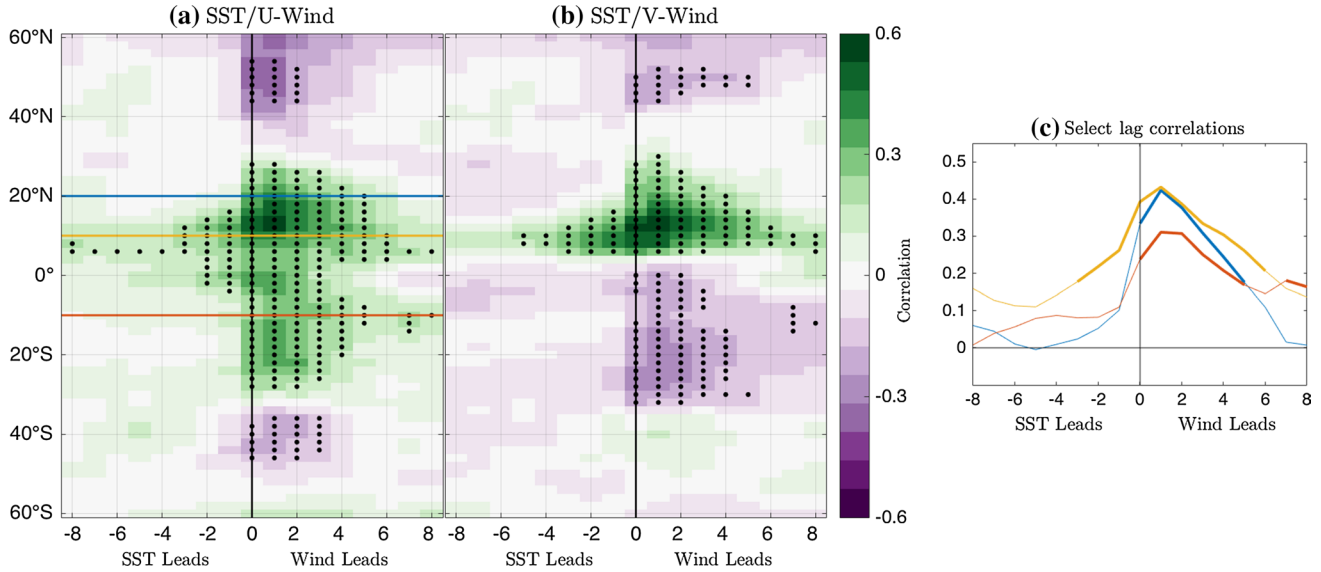

Fig. 4 **a** Lag correlation (*shading*) between the observed zonal mean SSTA and 10-m U-wind across the Atlantic basin. *Horizontal colored lines* indicate the select lag correlation curves shown in (**c**). **b** As in (**a**), but for the 10-m V-wind. **c** Select lag correlation curves at 20°N (*blue*), 10°N (*yellow*), and 10°S (*red*). *Stippling* in (**a**) and (**b**) and the *bold parts* of the curves in **c** indicates significance at 95% based on the e-folding timescale of the autocorrelation of the zonal mean SSTA at each latitude. The *vertical black line* denotes zero lag and the lags (shown on the x-axis) are in months

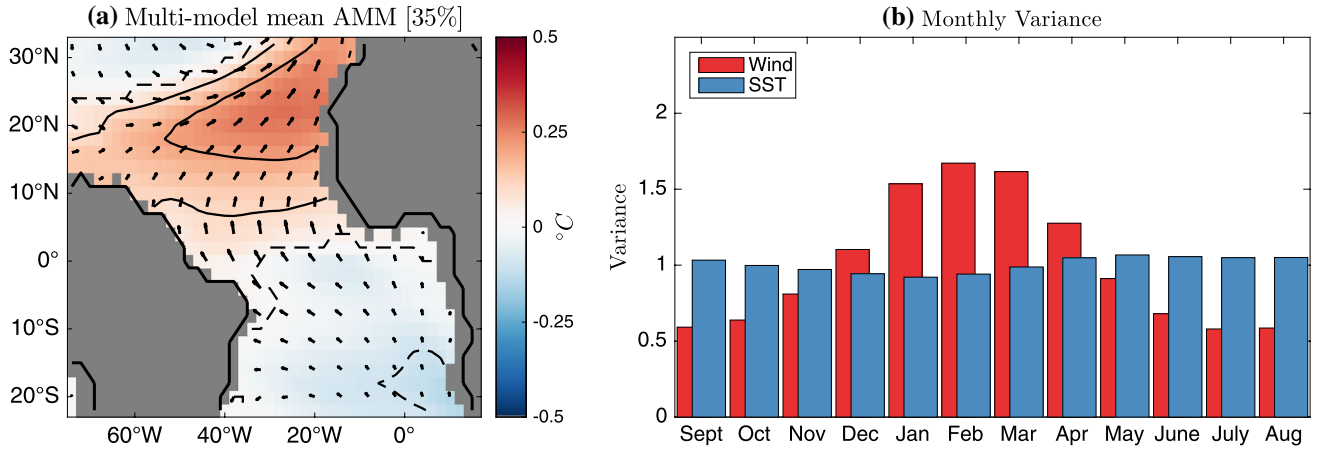

Fig. 5 As in Fig. 1a, c, but for the multi-model mean of the 17 CMIP5 models listed in Table 1. Note the different y-axis in (**b**)

atmosphere-forced temperature change and Newtonian cooling in the evolution of SSTAs that lie on the subtropical/tropical boundary (e.g., Xie 1999).

During JJA, the maximum SSTA propagates further southwestward and is now centered at 12°N, 50°W (Fig. 2c). There is continued evidence of a WES feedback from 10°N to 5°N and 50°W to 40°W, as anomalous southwesterly flow and negative latent heat flux anomalies are co-located with the southwestern edge of the SSTA maximum (green contour, Fig. 3c). However, in the absence of sustained atmospheric forcing, the SSTAs off the coast of Africa that were seen in DJF and MAM have weakened substantially due to the cooling associated with a continued upward flux of latent energy in that region (Fig. 3c).

Are the upward latent heat flux anomalies seen in MAM strong enough to account for the ~0.3 °C cooling observed from MAM to JJA near the African coast? A qualitative heat budget analysis can be analyzed to investigate the contribution of the latent heat flux to the mixed layer temperature change in this region. The change in SST from MAM to JJA, ΔSST, can be estimated as:

$$\Delta SST = \frac{\Delta t * Q_{LH}}{\rho C_p h} \quad (1)$$

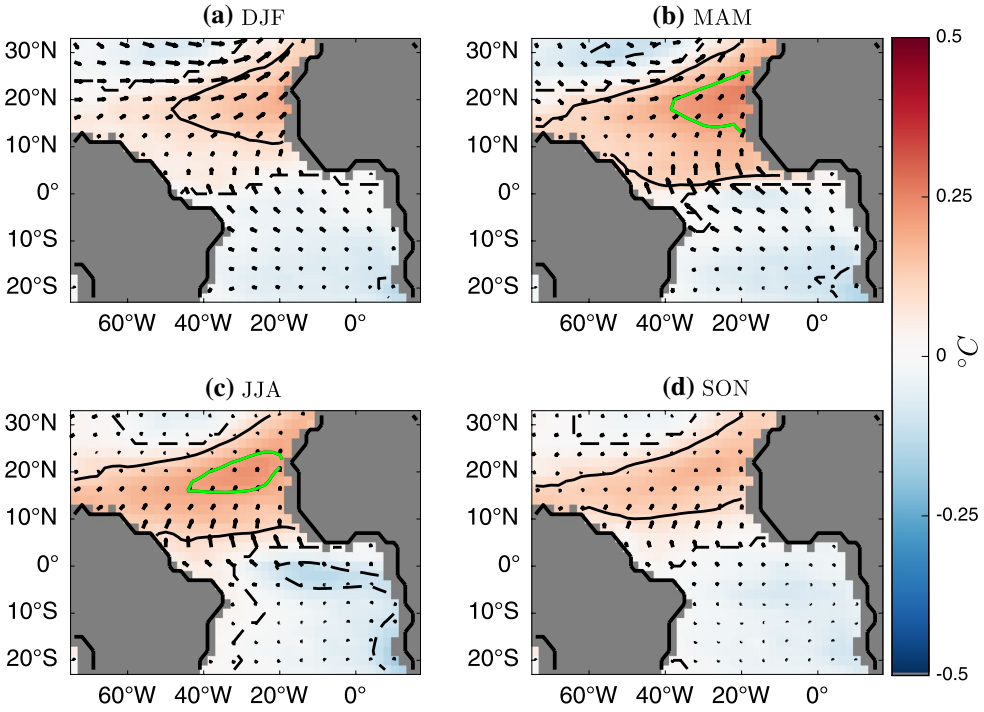

Fig. 6 As in Fig. 2, but for the multi-model mean of the 17 CMIP5 models listed in Table 1. The contour interval is 0.1 °C, but the *green line* now denotes the 0.2 °C contour

where the change in time, Δt, is three months, $\rho C_p = 4.088 \times 10^6$ J K^{-1} m^{-3}(Cronin et al. 2013), and $h \approx 30$ m (Foltz et al. 2013). The average latent heat flux, Q_{LH}, during MAM is -3.8 Wm^{-2} (negative because it is an energy gain for the atmosphere, but an energy loss for the ocean) from 20°N to 10°N, 30°W to 15°W. Using Eq. (1), we get an estimated $\Delta SST \approx -0.24$ °C, which corresponds well to the average ΔSST in that same box of -0.25 °C (not shown). The consistency of this rough estimate, based on a simple mixed-layer model approximation, is somewhat surprising when considering the potential impact of stratocumulous cloud and African dust forcing on SSTA via surface shortwave radiation in this region (e.g., Evan et al. 2013; DeFlorio et al. 2014). Therefore, while this preliminary calculation indicates that latent heat flux anomalies represent the main contribution to SST change from MAM to JJA, this may not necessarily be true for all of the north tropical Atlantic or for all seasons given that the mixed layer depth can vary in time and space by as much as 40 m (Foltz et al. 2013) and given the significant impact of other regional forcing terms on SSTAs (e.g., Evan et al. 2013; DeFlorio et al. 2014).

The anomalous surface flow and associated latent heat flux anomalies in SON are harder to interpret, as they are less spatially coherent and are not physically consistent with the temporal evolution of the AMM from DJF to JJA (Figs. 2d, 3d). However, the SON SSTA structure remains physically consistent with the energy fluxes from the previous season as the maximum SSTA propagates into the South American coastline and the SSTA spanning the rest of the basin decays further.

It should be noted that the physical mechanisms for SSTA growth, propagation, and decay described above were limited to the tropical north Atlantic region. The covariability in the tropical south Atlantic region does not evolve similarly and largely maintains southeasterly flow, negative SSTA, and positive latent heat flux anomalies throughout the year. The SH lobe of the AMM has been shown to be statistically independent of the NH lobe (e.g., Mehta and Delworth 1995; Enfield and Mestas-Nuñez 1999). Therefore, the spatiotemporal evolution of SH SSTA may be found in a higher order EMCA mode, or it may materialize if a different EMCA domain was chosen to emphasize SH coupled variability. We encourage future studies to further describe and understand this distinction.

4 Transition from atmosphere forcing ocean to ocean–atmosphere coupling

In Sect. 3, we used observations to demonstrate the importance of WES feedback in sustaining and propagating SSTAs from subtropical latitudes to the deep tropics. This process is dependent on the ocean's ability to force sufficiently strong low-level wind anomalies, which then feedback and significantly enhance the local SSTA. Without this ocean–atmosphere coupling, model analysis suggests that an SSTA generated at subtropical latitudes by stochastic atmospheric variability will not grow or propagate into tropical latitudes and become an AMM event (Chang et al. 2001; Chiang et al. 2002; Czaja et al. 2002). Therefore, it

is of interest to empirically identify the latitudes at which the climate regime shifts from atmosphere-forcing-ocean to full ocean–atmosphere coupling. Such an analysis would improve our understanding of where air-sea coupling occurs in the tropical Atlantic and may demonstrate to what extent the AMM acts as a connection between extratropical atmospheric variability and equatorial SST variability.

To help characterize this regime shift, we propose a symmetry index based on the lag correlation structure of Atlantic zonal mean SSTA and surface wind anomalies as a function of latitude. The more symmetric the lag correlation structure between the two variables, the greater the evidence for ocean–atmosphere interactions at that latitude. In contrast, strong asymmetries would be indicative of a one-way communication between the SST and surface winds. We calculate this symmetry index for zonal mean SST/U-wind anomalies and zonal mean SST/V-wind anomalies, respectively (Fig. 4a, b). Select lag correlations at 20°N (blue), 10°N (yellow), and 10°S (red) are shown in Fig. 4c. Stippling in Fig. 4a, b and the bold parts of the curves in Fig. 4c indicates statistical significance at 95%, which is based on the e-folding timescale of the autocorrelation function of the zonal mean SSTA at each latitude. The lags on the x-axis of each plot are in months.

Significantly negative correlations between SSTA and wind anomalies exist at 50°N–45 N° when the wind leads by 0–2 months for SST/U-wind and 0–5 months for SST/V-wind. A similar lobe of significantly negative correlations for SST/U-wind is found at southern midlatitudes, while SST/V-wind has positive correlations at positive lags that are not statistically significant. These four midlatitude lobes are consistent with an atmosphere-forcing-ocean climate regime (e.g., Alexander and Scott 1997) in which positive SSTAs are locally generated as a result of northerly and easterly wind anomalies in the NH and southerly and easterly wind anomalies in the SH.

Similar lag-lead relationships are evident in NH subtropical latitudes (30°N–20°N, Fig. 4). In this region, significant positive correlations can be found between SST and both components of the wind at lags ranging from 0 to 6 months. The lag correlation sign change is consistent with a shift in the background wind state from midlatitude westerlies to the northeasterly trade winds. The increase in the number of significant lags going southward from 30°N to 20°N is also likely due to this gradual shift from westerly to northeasterly flow. The magnitude of the background flow is weak at 30°N compared to 20°N, thus we would expect a weaker SSTA response for a given wind perturbation at 30°N relative to 20°N. This atmosphere-forcing ocean regime is consistent with NAO variability driving SST changes through surface heat fluxes (e.g., Chang et al. 2001).

For the deep tropical region of 20°N–0°, the lag correlation structure for the SST and both wind components are much more symmetric. In particular, significant positive correlations occur at large negative lags (when SSTAs lead wind anomalies) in a narrow meridional band ranging from 10°N to 6°N, where SST/U-wind has a significant correlation at all lags and SST/V-wind has a significant correlation at lags of −5 to 8 months. The tails at large negative and positive lags at these latitudes are remarkably consistent with the most significant southwesterly surface winds and negative latent heat flux anomalies found on the southwestern edge of the warm pool (green contour) depicted in Figs. 2b and 3b. Such symmetry in the lag correlation structure provides further evidence that air-sea interactions like WES feedback are significant contributors to SST and wind variability at these latitudes. The transition from an atmosphere-forcing-ocean environment to a two-way interaction is further highlighted by the select lag correlations depicted in Fig. 4c. The lag correlation at 20°N (blue) peaks at a lag of 1 month and drops sharply to zero for short negative lags, whereas the lag correlation at 10°N (yellow), although it also peaks at a lag of 1, has much stronger and more significant lag correlations at long negative lags.

The symmetrical lag correlation structures for SST/U-wind from 4°N to 4°S may be associated with Bjerknes feedback processes and the Atlantic Niño mode. Therefore, it is difficult to assess to what degree WES feedback dynamics contribute to the structure in this region. Additionally, although the SST/V-wind lag correlation structure near the equator is less likely to be impacted by Atlantic Niño, the climatological background wind here is usually small, so a meridional wind perturbation is less likely to produce a significant SSTA via WES interactions. This may explain why the SST/V-wind correlation is either zero or insignificantly negative from 4°N to 0°.

In the subtropics and deep tropics of the SH, the lag correlation structures for both SST/U-wind and SST/V-wind do not show a similar transition from atmosphere-forcing-ocean to ocean–atmosphere coupling compared to the NH. In particular, significant correlations between SST and U-wind only exist at positive lags from 6°S to 30°S, and at all southern latitudes for SST and V-wind. This relationship is emphasized by the 10°S curve (red) in Fig. 4c, which more closely resembles the northern subtropics than the northern tropics, albeit with weaker correlation values. The absence of significant correlations when the SST leads the wind in the SH tropics is puzzling and will be discussed in greater detail in Sect. 6.

5 CMIP5 evaluation

Tropical Atlantic coupled variability has not been extensively evaluated in CMIP5 models, with several exceptions. Liu et al. (2013) evaluated Atlantic warm pool variability

Table 2 The first column lists all datasets (observations and CMIP5 models) used in this study

	MCA (EMCA) AMM mode	Covariance explained (%) by MCA (EMCA) AMM	Pattern correlation coefficient b/w model MCA (EMCA) and observations
Observations	1 (1)	66 (49)	1 (1)
ACCESS1-0	2 (1)	21 (55)	0.57 (0.60)
ACCESS1-3	2 (1)	22 (33)	0.74 (0.61)
BNU-ESM	2 (2)	19 (16)	0.82 (0.78)
CNRM-CM5	1 (1)	50 (39)	0.79 (0.70)
GFDL-ESM2G	1 (1)	46 (32)	0.80 (0.67)
GFDL-ESM2M	2 (2)	18 (9)	0.68 (0.53)
INM-CM4	2 (2)	18 (15)	0.60 (0.65)
IPSL-CM5A-LR	2 (3)	33 (11)	0.68 (0.84)
IPSL-CM5A-MR	1 (1)	42 (34)	0.56 (0.74)
IPSL-CM5B-LR	1 (1)	71 (60)	0.81 (0.76)
MIROC5	1 (1)	44 (51)	0.58 (0.59)
MPI-ESM-LR	1 (1)	44 (38)	0.88 (0.74)
MPI-ESM-P	1 (1)	41 (31)	0.78 (0.58)
MRI-CGCM3	1 (2)	36 (21)	0.65 (0.67)
MRI-ESM1	1 (1)	43 (50)	0.72 (0.63)
NorESM1-M	1 (3)	42 (10)	0.73 (0.77)
NorESM1-ME	4 (4)	6 (5)	0.56 (0.61)
Multi-model mean	1.53 (1.65)	35.06 (30)	0.70 (0.67)

The second column is each model's MCA mode used in the multi-model mean for Fig. 5. The corresponding EMCA mode used in the multi-model mean for Figs. 6 and 7 is in parenthesis. The third column is the squared covariance fraction for the MCA (EMCA) mode indicated in the second column. The fourth column is the pattern correlation coefficient of the model MCA (EMCA) SSTA structure with the observed leading MCA (EMCA) mode. For the EMCA pattern correlation, the MAM SSTA structure was used. The last row is the average of each column, excluding the observations

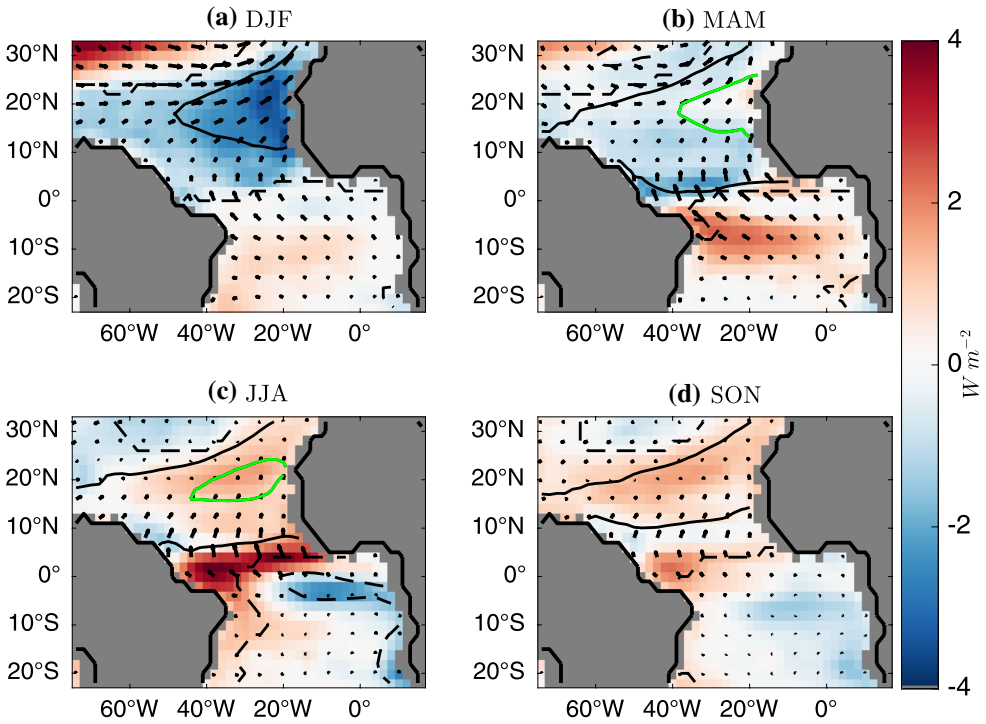

Fig. 7 As in Fig. 3, but for the multi-model mean of the 17 CMIP5 models listed in Table 1. The contour interval is 0.1 °C, but the *green line* now denotes the 0.2 °C contour. Note the *different color scale* between Figs. 3 and 7

in the historical simulations of 19 CMIP5 models, but stopped short of assessing the model's ability at reproducing coupled variability. Richter et al. (2014) analyzed CMIP5 model mean states and determined they exhibit too weak easterlies, and that the ITCZ is typically too far to the south. Given the significant impact of tropical Atlantic coupled variability on regional atmospheric circulation and precipitation, it is vital to assess the dexterity of CMIP5 models in reproducing observed coupled variability. Here, we repeat the observational analysis outlined in Sects. 3 and 4 on a suite of 17 CMIP5 models (Table 1). For brevity, we present only the results of the multi-model mean.

The multi-model mean AMM and the multi-model mean monthly variance of the respective ECs are shown in Fig. 5. It is important to note that unlike in observations, the leading mode of coupled variability in the CMIP5 models is not always the AMM. Therefore, to objectively determine the AMM mode for each model, we use a pattern correlation to compare the first five SSTA modes of the model MCA analysis to the observed AMM SSTA structure shown in Fig. 1. The model MCA mode with the highest pattern correlation was then selected to be the model's representation of the AMM and was included in the multi-model mean. A similar technique was used for the CMIP5 EMCA (Fig. 6), except the model AMM mode was found by comparing only the MAM SSTA structure between the models and observations. The mode number, the squared covariance fraction explained by each model's AMM, and the pattern correlation coefficient of each model's AMM with the observations for the CMIP5 MCA and EMCA analyses are listed in Table 2.

On average, the model AMM explains 35% of the covariance between tropical Atlantic SST and surface winds, which is only about half of the squared covariance fraction seen in the observations (Figs. 1, 5). The observed large-scale spatial structure of the AMM is generally well-reproduced in the CMIP5 models (Figs. 1a, 5a). There is a distinct interhemispheric SSTA gradient with a northeastward tilted warm lobe in the NH and general cooling in the SH. Additionally, surface wind anomalies are primarily southwesterly in the NH and southeasterly in the SH, with weak cross-equatorial flow. However, on average, the models generally underestimate the magnitude of the SSTAs, the meridional SSTA gradient, and the surface wind anomalies. This underestimation was also evident in CMIP3 models and could be related to well-known cold (warm) Atlantic SST biases in the NH (SH) (Liu et al. 2013).

Inspection of the multi-model mean month-to-month variance shows that the models reproduce the wind variability peak in January–February with reasonable accuracy. However, the multi-model mean wind variance is notably higher in boreal spring, while the observational variance declines sharply in March and April (Figs. 1c, 5b). Additionally, the models poorly simulate the observed peak of SST variability in the tropical Atlantic during MAM (Figs. 1c, 5b). Instead, the SST variance is lowest in boreal winter and roughly constant throughout the rest of the year. This discrepancy could be the result of a double ITCZ bias observed in CMIP5 models in the Atlantic (Richter et al. 2014). An incorrect representation of the lead-lag relationship of the atmosphere and ocean associated with the AMM may contribute to the inaccuracies seen in Fig. 5a. Further, inspection of power spectra based on each model's SST EC reveals that the models generally reproduce the observed interannual variability associated with the AMM, but tend to have more power at lower frequencies than seen in observations (not shown).

The multi-model mean EMCA of SSTA and surface winds is shown in Fig. 6, and the multi-model mean latent heat flux regression on to the respective EMCA SSTA ECs is shown in Fig. 7. Note that the green contour in Figs. 6 and 7 now represents the 0.2 °C contour. Similar to Fig. 5a, the CMIP5 models do a credible job in reproducing the observed genesis of the AMM SSTA structure, but the SSTA and wind anomaly magnitudes are once again underestimated (Figs. 2, 6). Additionally, the multi-model mean latent heat flux regression in DJF does not show the presence of the three distinct forcing regimes seen in observations (Figs. 3a, 7a). Instead, there are basin-wide negative latent heat flux anomalies from about 20°N–0° that are most consistent with the NAO-like forcing regime depicted in Fig. 3a, though they are much weaker than in observations (note the change in the color bar).

In MAM, the multi-model mean AMM peaks in strength, consistent with large negative latent heat flux anomalies seen in the previous season throughout the north tropical Atlantic from 20°N to 0°. These widespread negative latent heat flux anomalies have persisted into MAM, though they are weaker than in the winter. This broad swath of negative latent heat flux anomalies is also consistent with the NAO-like forcing regime and could be associated with the models producing springtime atmospheric forcing that is too large compared to observations, as indicated by the month–month variance analysis (Fig. 5b). Simultaneously, there is evidence of a weak ocean–atmosphere coupling with negative latent heat flux anomalies on the southwest edge of the warmest SSTAs and near-zero or slightly positive anomalies in the SSTA maximum (Figs. 6b, 7b). In the SH deep tropics, positive latent heat flux anomalies are co-located with negative SSTAs. These deep tropical latent heat flux anomalies in the model are consistent with being forced by model wind anomalies, which are southwesterly in the NH (albeit very weak) and southeasterly in the SH. Cross-equatorial flow also peaks during this season.

During JJA, the multi-model mean shows hints of seasonal SSTA propagation as indicated by the SSTA

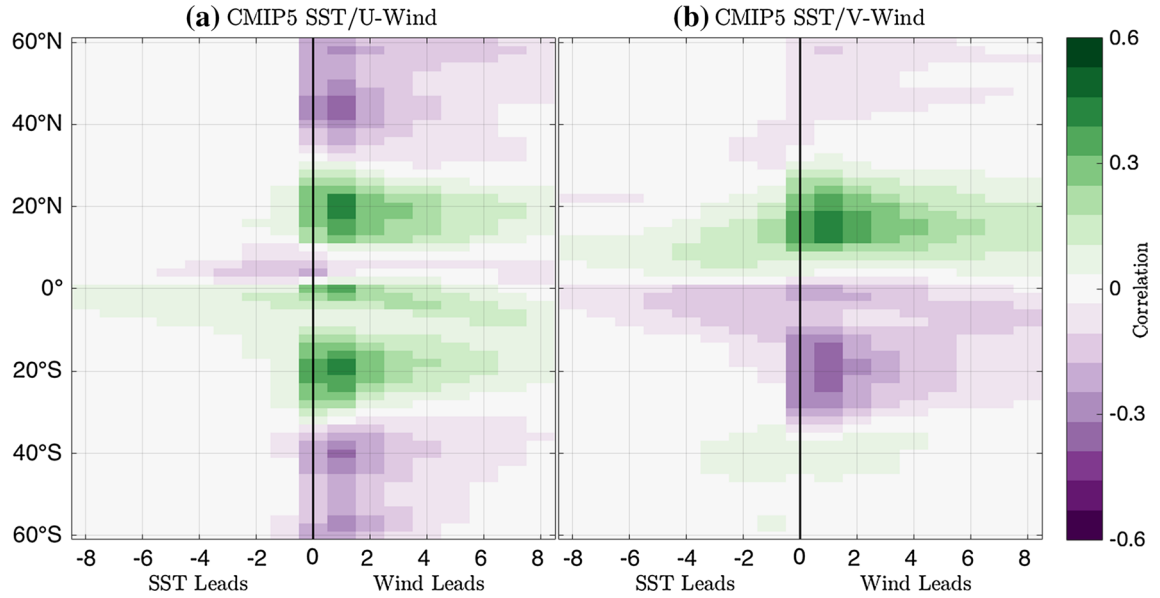

Fig. 8 As in Fig. 4a, b, but for the multi-model mean of the 17 CMIP5 models listed in Table 1

maximum outlined in green. However, it is clear from comparing Fig. 2b, c with Fig. 6b, c that the SSTA expansion from MAM to JJA is much less striking than in nature. The models' inability to reproduce significant SSTA propagation could be due to the fact that the most intense latent heat flux anomalies in the NH during MAM are found much closer to the equator and much further away from the edge of the SSTA warm pool relative to the observations. As a result, significant latent heat flux-driven SST change at the edge of the SSTA maximum may not occur, which would limit SSTA propagation in the models for the following season. Thus, while the multi-model mean representation of the AMM spatial structure is qualitatively consistent with observations shown in Figs. 2b and 3b, it is clear that the models' representation of the physical processes that govern WES feedback are not as spatially coherent.

It is also important to note that during JJA, the broad scale negative latent heat flux anomalies seen in the previous two seasons in the north tropical Atlantic have been replaced with nearly basin wide positive latent heat flux anomalies. The month-to-month surface wind variance analysis shows a marked decrease in magnitude during boreal summer. Thus, a reduction in atmospheric forcing in the absence of a robust WES feedback would allow for broad cooling of warm SSTAs associated with the model AMM, consistent with these broad upward latent heat flux anomalies (Figs. 5b, 7c).

Additionally, the multi-model mean EMCA shows a tongue of cold SSTAs on the equator in JJA that is not present in the observations. These cold anomalies are coupled with a zonal dipole of latent heat flux anomalies that is inconsistent with the cross-equatorial surface wind anomalies seen in Figs. 6c and 7c. The model latent heat flux response being more tightly confined to the equator is not simply the result of the multi-model mean smoothing over more varied behavior, but is a feature that exists in nearly all of the models (not shown). It is possible that the summertime EMCA in the models is being contaminated by overestimated Atlantic Niño variability or by the propensity for CMIP models to produce AMMs that have spuriously strong interactions with the Atlantic Niño (e.g., Breugem et al. 2006; Richter et al. 2014; Zebiak 1993).

The multi-model mean lag correlation between zonal mean SSTA and both wind components in the Atlantic as a function of latitude is shown in Fig. 8. The models credibly reproduce the SST/U-wind and SST/V-wind lag correlation structure at high latitudes. At both northern and southern mid-latitudes, the lag correlation is asymmetrical in favor of atmosphere forcing the ocean for the U-wind and V-wind, which is consistent with the observations (Figs. 4, 8). From 30° to 20° in both hemispheres, the modeled correlations continue to be realistic, and are consistent with stochastic atmospheric variability generating SST anomalies.

For SST/U-wind, the multi-model mean lag correlation structure and the observed lag correlation structure are dissimilar in the deep tropics. On average, the CMIP5 models do not accurately reproduce the observed transition from an asymmetrical atmosphere-forcing-ocean regime to a more symmetrical ocean–atmosphere coupled regime (Figs. 4a, 8a). Instead, the correlations from 10°N to 0°

become negative when the SST leads the winds, which is inconsistent with WES feedback processes. This is perhaps unsurprising given the model's difficulty in reproducing the observed spatial coherence of the latent heat and surface wind anomalies from season to season (Fig. 7). In contrast, the models tend to credibly simulate the lag correlation structure between the SSTAs and anomalies in the V-wind (Figs. 4b, 8b). Since the climatological surface winds at these latitudes are primarily zonal, perturbations in the U-wind component drive the most significant SSTA anomalies through WES dynamics (Xie 1999). Therefore, the inability of the CMIP5 models to reproduce the observed SST/U-wind lag correlation symmetry in the deep northern tropics may indicate that the models are incorrectly simulating air-sea coupling in this region. If the models are not producing a realistic WES interaction between the SST and the U-wind component, then this may help explain the poorly simulated propagation of SSTAs seen in Figs. 6 and 7.

6 Summary and discussion

In this study, the spatiotemporal evolution of SST and wind coupled variability in the tropical Atlantic was analyzed using observations and CMIP5 models. We confirm that the leading mode of observed coupled variability in the tropical Atlantic is the AMM, which explains 66% of the covariability. EMCA of seasonally stacked SST and surface wind anomalies was then utilized to depict a consistent and cohesive evolution of tropical Atlantic SSTAs from one season to the next in observations. In DJF, SSTAs are primarily forced by strong southwesterly surface wind anomalies, which reduce the strength of the background trade winds and reduce evaporative cooling at the surface, thereby warming the underlying ocean surface.

The regression of latent heat flux anomalies onto the EMCA SST EC during boreal spring provides evidence of air-sea coupling, and shows that the magnitude of the AMM peaks during this season. Additionally, near-zero surface wind anomalies and positive latent heat flux anomalies act as a damping on the warmest SSTAs, while strong southwesterly wind and negative latent heat flux anomalies are found along the southwest edge of the SSTA warm pool. This zonal dipole of latent heat flux and surface wind anomalies is consistent with WES feedback theory (e.g., Xie 1999). As a result of these energy fluxes, the SSTA maximum is driven southwestward into the South American coast during boreal summer and autumn.

A symmetry index based on the lagged temporal correlation between zonally averaged surface wind components and SST was then created to investigate the latitude at which tropical Atlantic air-sea coupling and WES feedback processes become the dominant mechanisms in driving SSTAs and surface wind anomalies. We show that the lag correlation structure at high latitudes is consistent with a white-noise atmosphere forcing strong SSTAs at positive lags. In the northern subtropics (30°N–20°N), the lag correlation structure is also dominated by an atmosphere-forcing-ocean regime. Further inspection of the northern deep tropics shows a smooth transition to more symmetric lagged temporal correlations, which is indicative of strong air-sea coupling. In particular, we identify a narrow region from 10°N to 6°N as having the most symmetrical lag correlations, which may indicate that air-sea interactions like WES feedback play the largest role in generating and maintaining SSTAs and surface wind anomalies at these latitudes.

We then evaluated the representation of tropical Atlantic coupled variability in a suite of CMIP5 models. The AMM spatial structure from the multi-model mean of the CMIP5 models is generally consistent with observations (Fig. 5). However, the models underestimate the magnitude of SST, surface wind, and latent heat flux anomalies throughout the basin. The model AMM errors could be a function of well-known SST biases throughout the tropical Atlantic (Richter et al. 2014; Liu et al. 2013), spurious relationships with Atlantic Niño (Breugem et al. 2006), or may perhaps be the result of issues in simulating the observed transition from an asymmetrical atmosphere-forcing-ocean environment to a more symmetrical ocean–atmosphere coupled environment.

In particular, the multi-model mean EMCA does not show a realistic southwestward propagation of the north tropical Atlantic SSTA maximum, which could be the result of the model's inability to correctly represent the spatial coherence of the physical processes governing WES feedback. As such, the ability of the average CMIP5 model to produce an AMM-like SSTA structure at all could be more due to boreal spring atmospheric forcing being too vigorous in the models (Figs. 1c, 5b). These overly strong westerly surface wind anomalies in spring may help explain the widespread negative latent heat flux anomalies seen in the models for DJF and MAM as well as the persistence of AMM-like SSTAs from one season to the next in spite of poorly representing WES feedback (Figs. 6, 7). It should be reiterated that these conclusions are drawn from the results of the multi-model mean analysis, and may smooth out more varied behavior among the models (not shown). Investigations into individual model performance and mean state biases should be pursued in future studies.

The results of this work bring together over two decades of research in tropical Atlantic variability and represent the first observational evidence for AMM growth, propagation, and decay driven by WES dynamics. This work also builds on the results of Chang et al. (2001) and others by

illustrating the meridional extent to which air-sea coupling becomes important in sustaining SSTAs in the tropical Atlantic. Further, these results enhance our understanding of how meridional modes act as bridges between subtropical atmospheric variability and deep tropical SST variability. This can be readily applied to investigate similar modes of coupled variability in other basins (e.g., PMM). Our analysis also includes the first assessment of a large ensemble of CMIP5 models in their ability to produce realistic air-sea interactions in the tropical Atlantic.

Several important questions arise from the results of our study. For example, what is the role of air-sea interactions in maintaining SSTAs in the south tropical Atlantic? Our observational analysis showed little evidence that ocean–atmosphere interactions drive significant SST or surface wind changes through WES feedback. One hypothesis that could explain the discrepancy between the hemispheres is the lower number of surface wind observations in the south Atlantic relative to the north Atlantic. However, when we repeat Figs. 2, 3, and 4 using reanalysis products that assimilate satellite scatterometry observations, we find that the SH still shows little indication of air-sea coupling in the deep tropics (not shown). This may be an indication that low-cloud SST feedbacks, which are independent of surface latent heat flux anomalies and surface wind convergences, are the dominant coupling mechanisms maintaining the SSTA in the SH (e.g., Evan et al. 2013; Tanimoto and Xie 2002).

It is also possible that the geometry of African coastline is unfavorable for WES feedback in the southeast Atlantic. In particular, the African continent at around 15°W limits the eastward extent of the warmest SSTA associated with the AMM. Therefore, the cross-equatorial surface wind anomalies forced by these SSTAs are limited to west of this longitude throughout the AMM's lifecycle (Figs. 2, 3). This leaves the southeast Atlantic (e.g., the Gulf of Guinea) in a shadow zone for anti-symmetric Rossby waves that help propagate the anomalies associated with WES feedback westward (e.g. Xie 2004). Further, CMIP5 multi-model mean SST/U-wind lag correlation structure was reproduced more accurately in the SH than in the NH (Fig. 8a). If we extrapolate the results of the NH and assume that the models poorly simulate air-sea interactions everywhere in the tropical Atlantic, then the fact that the models have skill in reproducing the SH SST/U-wind lag correlation may further highlight the insignificance of this type of air-sea interaction in generating and maintaining SH SSTAs. Based on this discussion, we feel a detailed investigation into the disparities between the NH and SH should be a focus of future work.

Coupled modes of tropical Atlantic variability like Atlantic Niño and the AMM are of high socioeconomic importance to the surrounding region. Therefore, future research efforts should build on the results of our observational analysis and aim to improve the representation of coupled interactions in climate models. Accomplishing this task would further enhance our understanding of air-sea interactions in the global tropics and increase our confidence in CMIP5 twenty-first century climate change projections.

Acknowledgements This material is based upon work supported in part by the National Science Foundation Graduate Research Fellowship (NSF; DGE-1144086). M.J.D is supported by the Jet Propulsion Laboratory at the California Institute of Technology, under a contract with the National Aeronautics and Space Administration. A.J.M is supported by the NSF (OCE1419306) and the National Oceanic and Atmospheric Administration (NOAA; NA14OAR4310276). S-P.X. is funded by the NSF Climate and Large Scale Dynamics Program 1305719, and NOAA Climate Program Office NA10OAR4310250. We would like to thank Daniel J. Vimont for his helpful comments during the course of our study. We also thank Yu Kosaka for downloading and processing the CMIP5 data presented in Table 1. ERSSTv3b data set is freely available and maintained by NOAA's National Climate Data Center. NCEP Reanalysis data was provided by the NOAA/OAR/ESRL PSD, Boulder, Colorado, USA, from their web site at http://www.esrl.noaa.gov/psd/. We also express our gratitude to the World Climate Research Programme's Working Group on Coupled Modelling, which maintains CMIP. Additionally, we thank the climate modeling groups listed in Table 1 for producing their model output and making it available. Finally, we thank two anonymous reviewers for comments that improved the quality of this paper.

References

Alexander MA, Scott JD (1997) Surface flux variability over the North Pacific and North Atlantic oceans. J Clim 10:2963–2978

Alexander MA, Vimont DJ, Chang P, Scott JD (2010) The impact of extratropical atmospheric variability on ENSO: testing the seasonal footprinting mechanism using coupled model experiments. J Clim 23(11):2885–2901

Amaya DJ, Foltz GR (2014) Impacts of canonical and Modoki El Niño on tropical Atlantic SST. J Geophys Res Oceans 119:777–789

Bretherton CS, Smith C, Wallace JM (1992) An intercomparison of methods for finding coupled patterns in climate data. J Clim 5:541–560

Breugem W-P, Hazeleger W, Haarsma RJ (2006) Multimodel study of tropical Atlantic variability and change. Geophys Res Lett 33(23). doi:10.1029/2006GL027831

Carton JA, Huang B (1994) Warm events in the tropical Atlantic. J Phys Oceanogr 24:888–903

Chang P, Ji L, Li H (1997) A decadal climate variation in the tropical Atlantic Ocean from thermodynamic air–sea interactions. Nature 385:516–518

Chang P, Ji L, Saravanan R (2001) A hybrid coupled model study of tropical Atlantic variability. J Clim 14:361–390

Chiang JC, Vimont DJ (2004) Analogous Pacific and Atlantic meridional modes of tropical atmosphere-ocean variability. J Clim 17:4143–4158

Chiang JC, Kushnir Y, Giannini A (2002) Deconstructing Atlantic ITCZ variability: influence of the local cross-equatorial SST gradient, and remote forcing from the eastern equatorial Pacific. J Geophys Res 107:4004

Cronin MF et al (2013) Formation and erosion of the seasonal thermocline in the Kuroshio Extension recirculation gyre. Deep-Sea Res II 85:62–74

Czaja A, van der Vaart P, Marshall J (2002) A diagnostic study of the role of remote forcing in tropical Atlantic variability. J Clim 15:3280–3290

DeFlorio MJ et al (2014) Semidirect dynamical and radiative effect of North African dust transport on lower tropospheric clouds over the subtropical North Atlantic in CESM 1.0. J Geophys Res Atmos 119:8284–8303

Di Lorenzo E, Mantua N (2016) Multi-year persistence of the 2014/2015 North Pacific marine heatwave. Nat Clim Change. doi:10.1038/nclimate308

Enfield DB, Mestas-Nuñez AM (1999) Multiscale variabilities in global sea surface temperatures and their relationships with tropospheric climate patterns. J Clim 12:2719–2733

Evan AT, Allan AJ, Bennartz R, Vimont DJ (2013) The modification of sea surface temperature anomaly linear damping time scales by stratocumulus clouds. J Clim 26:3619–3630

Folland CK, Palmer TN, Parker DE (1986) Sahel rainfall and worldwide sea temperatures, 1901–85. Nature 320:602–607

Foltz GR, McPhaden MJ (2010) Abrupt equatorial wave-induced cooling of the Atlantic cold tongue in 2009. Geophys Res Lett 37:L24605

Foltz GR, McPhaden MJ, Lumpkin R (2012) A strong Atlantic Meridional Mode event in 2009: the role of mixed layer dynamics. J Clim 25:363–380

Foltz GR, Schmid C, Lumpkin R (2013) Seasonal cycle of the mixed layer heat budget in the northeastern tropical Atlantic Ocean. J Clim 26(8169):8188

Frankignoul C, Kestenare E (2005) Air–sea interactions in the tropical Atlantic: a view based on lagged rotated maximum covariance analysis. J Clim 18:3874–3890

Frankignoul C, Kestenare E, Botzet M, Carril AF, Drange H, Pardaens A, Terray L, Sutton R (2004) An intercomparison between the surface heat flux feedback in five coupled models, COADS and the NCEP reanalysis. Clim Dyn 22:373–388

Hastenrath S, Heller L (1977) Dynamics of climatic hazards in northeast Brazil. Q J R Meteorol Soc 103:77–92

Kalnay E et al (1996) The NCEP/NCAR 40-year reanalysis project. Bull Am Meteorol Soc 77:437–471

Larson SM, Kirtman BP (2014) The Pacific meridional mode as an ENSO precursor and predictor in the North American multimodel ensemble. J Clim 27:7018–7032

Liu H, Wang C, Lee S-K, Enfield DB (2013) Atlantic warm pool variability in the CMIP5 simulations. J Clim 26:5315–5336

Mehta VM, Delworth T (1995) Decadal variability of the tropical Atlantic Ocean surface temperature in shipboard measurements and in a global ocean–atmosphere model. J Clim 8:172–190

Nobre P, Shukla J (1996) Variations of sea surface temperature, wind stress, and rainfall over the tropical Atlantic and South America. J Clim 9:2464–2479

Okumura Y, Xie S-P, Numaguti A, Tanimoto Y (2001) Tropical Atlantic air-sea interaction and its influence on the NAO. Geophys Res Lett 28:1507–1510

Polo I, Rodríguez-Fonseca B, Losada T, García-Serrano J (2008) Tropical Atlantic Variability Modes (1979–2002). Part I: time-evolving SST modes related to West African rainfall. J Clim 21:6457–6475

Richter I, Xie S-P, Behera S, Doi T, Masumoto Y (2014) Equatorial Atlantic variability and its relation to mean state biases in CMIP5. Clim Dyn 42:171–188

Ruiz-Barradas A, Carton JA, Nigam S (2003) Role of the atmosphere in climate variability of the tropical Atlantic. J Clim 16:2052–2056

Smith TM et al (2008) Improvements to NOAA's historical merged land-ocean surface temperature analysis (1880–2006). J Clim 21:2283–2296

Sutton RT, Jewson SP, Rowell DP (2000) The elements of climate variability in the tropical Atlantic region. J Clim 13:3261–3284

Tanimoto Y, Xie S-P (2002) Inter-hemispheric decadal variations in SST, surface wind, heat flux and cloud cover over the Atlantic Ocean. J Meteorol Soc Jpn 80:1199–1219

Vimont DJ (2010) Transient growth of thermodynamically coupled variations in the tropics under an equatorially symmetric mean state. J Clim 23:5771–5789

Vimont DJ, Kossin JP (2007) The Atlantic Meridional Mode and hurricane activity. Geophys Res Lett 34:L07709

Vimont DJ, Battisti DS, Hirst AC (2001) Footprinting: a seasonal connection between the tropics and mid-latitudes. Geophys Res Lett 28:3923–3926

Vimont DJ, Wallace JM, Battisti DS (2003) The seasonal footprinting mechanism in the Pacific: implications for ENSO. J Clim 16:2668–2675

Vimont DJ, Alexander M, Fontaine A (2009) Midlatitude excitation of tropical variability in the pacific: the role of thermodynamic coupling and seasonality. J Clim 22:518–534

Wu S, Wu L, Liu Q, Xie S-P (2010) Development processes of the tropical Pacific meridional mode. Adv Atmos Sci 27:95–99

Xie S-P (1999) A dynamic ocean–atmosphere model of the tropical Atlantic decadal variability. J Clim 12:64–70

Xie S-P (2004) The shape of continents, air-sea interaction, and the rising branch of the Hadley circulation. In: Diaz HF, Bradley RS (eds) The Hadley circulation: past, present and future. Kluwer Academic, Dordrecht, pp 121–152

Xie S-P, Carton JA (2004) Tropical Atlantic variability: patterns, mechanisms, and Impacts. In: Wang C, Xie S-P, Carton JA (eds) Earth's climate. American Geophysical Union, Washington, D. C.

Xie S-P, Philander SGH (1994) A coupled ocean-atmosphere model of relevance to the ITCZ in the eastern Pacific. Tellus 46:340–350

Zebiak SE (1993) Air–sea interaction in the equatorial Atlantic region. J Clim 6:1567–1586